

Published in final edited form as:

*Mol Cell Neurosci.* 2009 December ; 42(4): 382–390. doi:10.1016/j.mcn.2009.08.010.

## Role of VASP phosphorylation for the regulation of microglia chemotaxis via the regulation of focal adhesion formation/maturation

S. Lee and C. Y. Chung\*

Department of Pharmacology, Vanderbilt University Medical Center, Nashville, TN 37232-6600

### Abstract

Microglia activation and migration are known to play crucial roles for the response to brain injuries. Extracellular ADP was reported to induce microglia chemotaxis and membrane ruffles through P2Y<sub>12</sub> receptor. In this study, we examined the role of VASP phosphorylation in ADP-induced microglia chemotaxis and membrane ruffle formation. ADP stimulation transiently increased intracellular cAMP level, VASP phosphorylation at Ser153, membrane ruffle formation, and chemotaxis. PKA inhibitor effectively inhibited VASP phosphorylation and chemotaxis, indicating that P2Y<sub>12</sub>-mediated activation of PKA and subsequent VASP phosphorylation are involved in the regulation of microglia chemotaxis. Forskolin and Okadaic acid induced sustained VASP phosphorylation at high level, causing a significant reduction of the retraction of membrane ruffles and chemotaxis. In Forskolin- or Okadaic acid-treated cells, phosphorylated VASP remained at the membrane cortex and size and number of mature focal adhesions was not increased, indicating that prolonged phosphorylation of VASP could inhibit transformation of focal complexes into focal adhesions. VASP knock-down cells showed markedly reduced frequency and distance of membrane ruffling upon ADP stimulation, reinforcing the idea that VASP is required for the ruffle formation. Cells expressing GFP-VASP<sup>S153A</sup> also showed a significant reduction of protrusion distance during ruffle formation, but the frequency and distance of retraction was not affected by FSK at all. This result suggests that dephosphorylation of VASP might be required for the growth of adhesion strength during membrane retraction. Our results suggest that VASP phosphorylation by PKA plays an important role in membrane ruffle formation and chemotaxis via the regulation of focal adhesion formation/maturation.

### Keywords

VASP; chemotaxis; microglia; focal adhesion

### INTRODUCTION

Microglia are the immune effector cells in the central nervous system (CNS). They play a crucial role in recognition and phagocytic removal of degenerating neurons (Hickey, 2001; Streit, 2002). The ramified morphology of resting microglia is transformed into a motile amoeboid form after pathological stimuli and migrates toward lesion sites, where they become activated and exert their neuroprotective effects such as secreting a variety of substances and clearing cell debris (Hanisch, 2002; Kreutzberg, 1996; Stence et al., 2001; Thomas, 1999). But their hyperactivation often leads to neurotoxicity and several neurodegenerative diseases accompanied by an excess proliferation of microglia (Gehrmann

---

Address correspondence to: Chang Y. Chung, 468 Robinson Research Building (MRB I), 1215 21<sup>st</sup> Ave. South @ Pierce, Nashville, TN 37232-6600; Phone: 615-322-4956; Fax: 615-343-6532; chang.chung@vanderbilt.edu.

et al., 1995). Thus, better understanding of the regulation of microglia proliferation and chemotaxis may have important therapeutic implications. However, the intracellular signals underlying microglia migration are poorly understood.

Microglia are known to express both ionotropic (P2X) and metabotropic (P2Y) purinergic receptors that have been proposed to have important roles in activation, motility, and paracrine signaling of these cells (Honda et al., 2001) (Inoue, 2002) (Sasaki et al., 2003). In brain with damaged neurons and astrocytes, large amounts of nucleotides are released from these cells (Dubyak and el-Moatassim, 1993; Neary et al., 1994). Extracellular ATP or ADP released from damaged cells and surrounding astrocytes could induce microglia chemotaxis and membrane ruffling through Gai/o-coupled P2Y<sub>12</sub> receptor in cultured rat microglia (Davalos et al., 2005; Haynes et al., 2006; Nimmerjahn et al., 2005) (Nasu-Tada et al., 2005) (Ohsawa et al., 2007). It has been reported that ATP-induced membrane ruffling is not dependent on PI3K activation, whereas the ATP gradient-dependent cell migration requires PI3K activation (Ohsawa et al., 2007). cAMP-elevating agents have been reported to inhibit ADP-induced microglia chemotaxis and membrane ruffling (Nasu-Tada et al., 2005). However, signaling pathways downstream of P2Y<sub>12</sub>R during chemotaxis are not fully understood. There is a growing body of evidence that extracellular matrix (ECM) and integrins are important for modulating microglial behavior. Fibronectin promoted transformation of amoeboid microglia into ramified microglia whereas laminin caused reverse transformation (Chamak and Mallat, 1991). It has been demonstrated that microglia attach well to fibronectin and vitronectin, but only weakly to laminin and astrocyte ECM. Furthermore, laminin exerts a dominant anti-adhesive effect on microglial adhesion (Milner and Campbell, 2002).

To better understand the regulation of adhesion and chemotaxis by ADP-induced intracellular signaling in microglia, we, in this study, examined the role of VASP phosphorylation by PKA in microglia adhesion and chemotaxis. We demonstrated that ADP stimulation caused the elevation of intracellular cAMP concentration. Inhibition of PKA or over-activation of PKA inhibited chemotaxis and membrane ruffle formation induced by ADP stimulation. Prolonged phosphorylation of VASP causes impaired focal adhesion formation/maturation and ruffle formation.

## MATERIALS AND METHODS

### Cell culture

BV2 microglial cells were maintained in Dulbecco's modified Eagle's medium (DMEM) (Gibco BRL, Grand Island, NY, USA) supplemented with 10% fetal bovine serum (FBS) (Gibco BRL) and penicillin-streptomycin (Gibco BRL). For each experiment, subconfluent cell cultures were harvested with trypsin and rinsed with DMEM medium containing 10 % FBS. MISSION shRNA clone (NM\_009499.1-28s1c1 from Sigma) containing hairpin sequences (CCGGCGGGCTACTGTGATGCTTTATCTCGAGATAAAGCATCACAGTAGCCCGTT TTTG) was used for VASP knockdown.

### Migration Assays

Migration assays were performed as previously described (O'Connor et al., 1998). Briefly, Transwell chamber membranes (6.5-mm diameter, 8- $\mu$ m pore size, Corning, Corning, NY) were coated with 3 or 20  $\mu$ g/ml of fibronectin for 8 hr (Sigma, St. Louis, MO). For chemotaxis assays, either serum-free DMEM medium or serum-free DMEM containing 100  $\mu$ M adenosine 5'-diphosphate (ADP) (Sigma) was added to the lower chamber. Cells ( $1 \times 10^4$ ) suspended in serum-free DMEM were added to the upper chamber. The effect of

the several kinase inhibitors, P2Y<sub>12</sub> receptor antagonist or cAMP-elevating agents - LY294002 (Promega, Madison, WI) (20  $\mu$ M), H-89 (Sigma) (30  $\mu$ M), Y-27632 (Alexis, San Diego, CA) (10  $\mu$ M), Dimethylthioadenosine 5'-monophosphate (Sigma) (2MeSAMP) (50  $\mu$ M) and Forskolin (Sigma) (FSK) (10  $\mu$ M) - were added to the upper chamber. After incubating for 4 hr at 37°C, nonmigrating cells were removed from the upper chamber with a cotton swab and cells that had migrated to the lower surface of the membrane were fixed with 3.7% formaldehyde for 10 min and stained with 0.2% crystal violet. Images were captured with Roper Coolsnap camera (Tucson, AZ) and Metamorph software (Universal Imaging, West Chester, PA). Migration was quantified using Image Quant software (Molecular Dynamics, Sunnyvale, CA).

### Membrane ruffling

Membrane ruffling was performed as previously described (Borm et al., 2005a). Live-cell membrane ruffling was performed on a Nikon TE2000 microscope at 37°C with Hamamatsu Orca-ER camera and Metamorph software. For phase-contrast microscopy, cells were attached to glass coverslips (Fisher, Fair Lawn, NJ) coated with 3  $\mu$ g/ml or 20  $\mu$ g/ml of fibronectin. After attachment for overnight, cells were washed with serum-free DMEM and starved for 4 hr in the same medium. For single-cell ruffle formation studies, images were taken with a 10 $\times$ 0.30 plan neofluar Ph1 objective lens. Lamella dynamics and cell migration velocity were analyzed by the kymographic assay (Bear et al., 2002). For each group, at least 10 individual cells were monitored over a 15 min period by capturing digital images every 6 sec. Subsequently, three areas of interest were marked on each image by lines that cross the cell lamella. Kymographs were analyzed with Metamorph and Excel software. Kymographs are composite time-space images of membrane movement at a single point of an actively protruding lamellipod, created by extracting image information from a defined line region in each image of a time-lapse movie and pasting them side-by-side.

### Immunofluorescence staining and F-actin staining

Cells were attached to glass coverslips (Fisher) coated with 3  $\mu$ g/ml of fibronectin. After attachment for overnight, cells were washed with serum-free DMEM and starved for 4 hr in the same medium. They were then stimulated with 5  $\mu$ M ADP for 5 min at 37°C. In the control, cells were treated with phosphate buffered saline (PBS) or DMSO instead of ADP or inhibitors. The reaction was stopped by the addition of PBS containing 3.7% formaldehyde. After fixation for 10 min and washing with PBS, the cells were permeabilized with PBS containing 0.2% Triton X-100 for 10 min and washed three times with PBS. And then non-specific binding was blocked with blocking solution containing 1% bovine serum albumin (BSA) in PBS for 10 min. To visualize paxillin and actin, the cells were stained for 1 hr with anti-mouse paxillin (diluted 1:1,000, BD Biosciences, San Jose, CA). Cells were then incubated with TRITC-labeled phalloidin (Sigma) and FITC conjugated goat-anti mouse IgG (Santa Cruz, Santa Cruz, CA) in 5% BSA in PBS for 1 hr. Images were captured with Roper Coolsnap camera and Metamorph software. The effect of the inhibitors or agonist were assessed by preincubating cells with LY294002 (Promega) (20  $\mu$ M), H-89 (Sigma) (30  $\mu$ M) for 20 min, Dimethylthioadenosine 5'-monophosphate (Sigma) (2MeSAMP) (50  $\mu$ M) for 5 min, Y-27632 (Alexis, San Diego, CA) (10  $\mu$ M) for 1 hr and cAMP-elevating agents Forskolin (Sigma) (FSK) (10  $\mu$ M) for 30 min, and then stimulating them with ADP.

## RESULTS

### ADP-induced cell migration and membrane ruffling of microglia are through G<sub>i/o</sub>-coupled P2Y<sub>12</sub> receptor

A previous study reported that extracellular ATP or ADP could induce PI3 kinase activation and chemotaxis of microglia via the G<sub>i/o</sub>-coupled P2Y<sub>12</sub> receptor (Honda et al., 2001; Inoue, 2002; Ohsawa et al., 2007). To understand the intracellular signaling pathway downstream of P2Y<sub>12</sub> receptor underlying microglial chemotaxis, we examined the activation of PI3 kinase and chemotaxis in cells stimulated with ADP. ADP stimulation significantly increased the level of Akt phosphorylation at Ser<sup>473</sup> and Thr<sup>308</sup> (Fig. 1A). Pretreatment of cells with 2-methylthio-AMP 2-methylthio-AMP (2MeSAMP, a P2Y<sub>12</sub> antagonist), Pertussis Toxin (PTx), and LY294002, a general PI3 kinase inhibitor, caused a significant inhibition of Akt phosphorylation at both Ser<sup>473</sup> and Thr<sup>308</sup>. However, pretreatment with AS604850, a PI3K $\gamma$  specific inhibitor, inhibited Akt phosphorylation only at Thr<sup>308</sup>. Chemotaxis of BV2 microglia cells were assessed by using a transwell assay. In the absence of the ADP, microglia did not migrate in the fibronectin-coated transwell chamber whereas cells showed a significant migration toward the lower chamber containing 100  $\mu$ M ADP (Fig. 1B). No significant increase of chemotaxis was observed when ADP was added to the lower and upper chamber, ruling out the possibility of chemokinesis. Cells treated with PTx (100 ng/ml) and 2MeSAMP (50 $\mu$ M) showed significant inhibition of ADP-induced chemotaxis. Pretreatment of the microglia with LY294002 also significantly blocked the chemotaxis. However, AS604850 showed a moderate inhibition of the ADP-induced chemotaxis, suggesting that there might be subtype-specific roles of PI3 kinases. The ruffling of the plasma membrane is the formation of motile cell surface protrusions containing a meshwork of newly polymerized actin filaments and is a characteristic feature of many actively migrating cells (Borm et al., 2005b). A previous study reported that extracellular ATP and ADP induced membrane ruffling through P2Y<sub>12</sub> receptor (Honda et al., 2001). However, membrane ruffles were examined only by phalloidin staining. To elucidate how dynamic regulation of ruffle formation is controlled by P2Y<sub>12</sub> receptor signaling, we examined membrane ruffling formation induced by ADP using a video microscopy over a 15 min period after ADP treatment. These time-lapse videos were analyzed by kymography, a technique that allows for the quantitation of frequency and distance of membrane protrusion and retraction. Multiple areas of interest in a cell were marked by lines crossing the cell lamella, and kymographs were created to examine the frequency and distance of membrane ruffles. Both frequency and distance of membrane protrusion and retraction are greatly enhanced after ADP treatment (Fig. 1C). However, PTx and 2MeSAMP significantly inhibited ADP-induced membrane ruffle formation. LY294002 also inhibited membrane ruffle formation. Interestingly, AS604850 did not show a significant inhibition of ruffle formation, consistent with moderate inhibition on the phosphorylation on Thr<sup>308</sup> and chemotaxis. These results suggest that PI3K $\gamma$  might have a less important role in the regulation of microglia chemotaxis.

### PKA activity is required for ADP-induced chemotaxis and membrane ruffle formation

In a previous study (Nasu-Tada et al., 2005), cAMP-elevating agents such as forskolin or dibutyryl cAMP were reported to inhibit ADP-induced membrane ruffling and chemotaxis, indicating that PKA activation might have a negative effect on ADP-induced cell migration. However, it is still not clear how PKA activation causes inhibition of chemotaxis of microglia towards cAMP. To elucidate a mechanism, we first determine if ADP could affect adenylyl cyclase (AC) activity in microglia through G<sub>i/o</sub>-coupled P2Y<sub>12</sub> receptor. Changes of intracellular cAMP concentration upon ADP stimulation was measured using a Catchpoint cAMP assay kit (Molecular devices). Intracellular cAMP concentration appears to be elevated by ADP, reaching maximum concentration of 3.3 nM at 5 min after ADP

stimulation (Fig. 2A). Folskolin (FSK), an AC-activating agent, also caused the elevation of cAMP to a comparable level and cAMP concentration was further elevated in cells treated with both FSK and ADP (Fig 2B). Cells treated with 2MeSAMP showed significantly lower AC activation upon ADP stimulation whereas LY294002 exhibited minimal inhibition. These results suggest that ADP induces AC activation through  $G_{i/o}$ -coupled P2Y12 receptor. ADP is an agonist of P2Y1, P2Y12, and P2Y13 receptors (Van Kolen and Slegers, 2006). P2Y1 has been reported to be  $G_q/G_{11/12}$ -coupled receptor while P2Y12 and P2Y13 are coupled to  $G_i$ . To examine if P2Y1 might be involved in the AC stimulation, we used MRS 2179, a specific inhibitor for P2Y1 receptor and it did not show any inhibition of AC stimulation by ADP. This result again indicates AC activation through  $G_{i/o}$ -coupled P2Y12 receptor. Elevation of cAMP concentration upon ADP stimulation presumably causes an activation of cAMP-dependent protein kinase (PKA). To determine whether PKA activation is required for chemotaxis and membrane ruffle formation, we investigated the effects of H-89, a PKA inhibitor. Cells treated with 30  $\mu$ M H-89 exhibited significantly reduced ADP-induced ruffle formation (Fig. 2C) as both frequency and distance of membrane protrusion and retraction were markedly reduced. Interestingly, increase of adhesion strength with higher FN coating concentration (20  $\mu$ g) affects frequency and distance of membrane ruffling. Lamellipodia at the lower amount of FN (3  $\mu$ g) exhibited oscillating waves of protrusion and retraction of membrane upon ADP stimulation whereas lamellipodia at the higher amount exhibited more frequent protrusions and retractions with similar distance to 3  $\mu$ g of FN. Increase of adhesion strength partially rescues membrane ruffling defects in cells treated with H-89, indicating that cell-adhesion strength might play an important role for the regulation of ruffling dynamics. Cells treated with FSK, however, showed a somewhat different defect of ruffle formation. As shown in kymographs (Fig. 2C), a long protrusion with rare retraction was a dominant form of ruffle in FSK-treated cells. Increase of adhesion strength again rescued defects of ruffling caused by FSK. We reasoned that FSK might induce prolonged phosphorylation of protein(s) and prevention of dephosphorylation by inhibiting a PP2A activity by OA might have the same effect on ruffle formation. Indeed, cells treated with OA showed almost identical defect of ruffle formation to cells treated with FSK and this defect could be reversed by the increase of adhesion strength. These results suggested that PKA activation is needed for membrane protrusion formation and the effect of FSK or OA is dependent on the strength of cell adhesion. We examined chemotaxis of these cells in transwell to determine how defects of ruffle formation affect chemotaxis. H-89, FSK, and OA showed strong inhibition of chemotaxis and, unlike ruffle formation, increase of adhesion strength partially rescued only chemotaxis of cells treated with FSK (Fig. 2D). These results suggest that variations in cell-substratum adhesion strength can affect the directional persistence of cell paths through modulation of the stability of short-timescale local membrane protrusion events.

Adhesion strength of cells are dependent upon the number and size of focal adhesions (Critchley, 2000). Previous reports indicated that the focal complexes (FX) are involved in protrusion formation at the leading edge, and the focal adhesions (FA) are involved in the contractile actomyosin system to pull the cell body and restrain the migration process (Zimmerman et al., 2004). Paxillin is a multi-domain protein and a major component of focal complex and adhesion. To determine changes of focal complex and adhesion, we examined immunostaining of paxillin. Upon ADP stimulation, the number of focal adhesions and stress fibers was markedly increased up to three times and the size was also increased (Fig. 3A). Cells plated on 20  $\mu$ g of FN showed twice as many focal adhesions as cells plated on 3  $\mu$ g, and the number was increased to the level of ADP-stimulated cells plated on 3  $\mu$ g (Fig. 3B). The average size of focal adhesions in cells plated on 20  $\mu$ g of FN was 2.3  $\mu$ m<sup>2</sup> which is similar to the size of focal adhesions in cells stimulated with ADP. These results clearly indicate that cells plated on higher concentrations of FN have more and bigger focal adhesions, suggesting stronger adhesion. H-89 showed a strong inhibitory effect

on the increase of focal adhesion numbers and size upon ADP stimulation as cells showed significantly decreased number of focal adhesions (Fig. 3B). This result suggests that PKA activity is required for the increase of the number and size of focal adhesions. Cells treated with FSK or OA showed significantly decreased number of focal adhesions and the size of focal adhesions was also moderately decreased in these cells. Interestingly, there was a significant increase of paxillin localization to the focal complexes at the cortex of ruffling membranes in these cells at the expense of focal adhesions. Cells plated on 20  $\mu$ g of FN showed significant recovery of adhesion numbers, but not the size, even in the presence of FSK or OA, suggesting that adhesion strength plays an important role for the maturation of small focal complexes into focal adhesions.

VASP is a major substrate for PKA and it is localized to focal adhesions and areas of dynamic membrane activity (Krause et al., 2003). It is plausible that VASP phosphorylation by PKA activation upon ADP stimulation might play an important role in controlling membrane ruffling and focal adhesions. Thus, we first determined if ADP induced VASP phosphorylation through  $G_{i/o}$ -coupled P2Y<sub>12</sub> receptor in microglia. VASP phosphorylation at Ser<sup>153</sup> was increased significantly upon ADP stimulation. As expected, PTx, 2MeSAMP, and H-89 inhibited ADP-induced VASP phosphorylation (Fig. 4A), indicating VASP phosphorylation through  $G_{i/o}$  coupled receptor and PKA signaling. MRS2179, a P2Y<sub>1</sub> antagonist, did not show any significant inhibition of VASP phosphorylation while MRS2211, a P2Y<sub>13</sub> antagonist, caused moderate inhibition of VASP phosphorylation. We also tested if VASP phosphorylation was regulated by PKG activation through P2Y<sub>12</sub> receptor. We used a PKG inhibitor, DT-2, which did not inhibit ADP-induced VASP phosphorylation (data not shown). FSK and OA increased VASP phosphorylation in a dose-dependent manner up to the level comparable to cells treated with ADP (Fig. 4A). FSK and ADP together further increased VASP phosphorylation. Therefore, the level of P-VASP closely follows changes in intracellular cAMP concentration. To better understand the function of VASP phosphorylation in the formation of membrane ruffles and focal adhesions, we determined the localization of phosphorylated VASP (pVASP) and paxillin after ADP stimulation by immunostaining. In quiescent, serum-deprived BV2 cells, paxillin localization is mainly to focal complexes or small focal adhesions near the membrane and pVASP was not readily detected (Fig. 4B). ADP stimulation induced not only the localization of paxillin to small focal complexes at the cortex of ruffling membranes but also a significant increase of pVASP localization to the cortex of ruffling membrane. FSK and OA along with ADP further increased the localization of pVASP and paxillin to the membrane, suggesting that VASP phosphorylation might be required for formation of focal complexes during the protrusion of membrane ruffles and prolonged VASP phosphorylation by FSK or OA might inhibit the maturation/growth of focal adhesions causing reduction of ruffle retraction.

To elucidate the role of VASP for microglia chemotaxis further, we created two cell lines, one that VASP expression was knocked down by transducing a lentivirus transfecting vector expressing a short hairpin VASP RNAi (shVASP) and the other expressing unphosphorylatable VASP mutant (GFP-VASP<sup>S153A</sup>). VASP protein expression examined by western blot was markedly suppressed in the VASP knock down (VASP-KD) cells (Fig. 5A). VASP knockdown cells showed markedly reduced frequency and distance of membrane ruffling (Fig. 5A), suggesting that VASP is required for the ruffle formation upon ADP stimulation. Reduction of ruffle formation appears not to be due to defects of F-actin polymerization in ruffling membranes since F-actin polymerization was largely unaffected in the VASP knock down cells (Data not shown). Cells expressing GFP-VASP<sup>S153A</sup> also showed a significant reduction of protrusion distance during ruffle formation, but the frequency of ruffling was not largely affected and, more importantly, the retraction frequency was not affected by FSK at all. This result suggests that dephosphorylation of

VASP might be required for the growth of adhesion strength during membrane retraction. To determine whether VASP is involved in the regulation of adhesion formation and/or disassembly in microglia, cells were transfected with GFP-paxillin which marks focal adhesions and allows quantitation of the rates of adhesion assembly (Fig. 5B). GFP-paxillin localized to prominent peripheral adhesion structures in both control and VASP-KD cells. The fluorescence intensity of GFP-paxillin in focal adhesions was measured by time-lapse microscopy and image analysis. To quantify dynamic changes of adhesions, the kinetics of adhesion formation was determined by integrating the fluorescent intensity in individual adhesion over time (Fig. 5C). Analysis of rate of fluorescent intensity changes in cells revealed that VASP-KD cells have a significantly slower assembly rate of focal adhesions formed within 1  $\mu\text{m}$  of the cell edge, consistent with the lack of mature, large focal adhesions away from the membrane in VASP-KD cells. VASP-KD cells showed significantly reduced chemotaxis towards ADP compared to control cells. Cells expressing GFP-VASP<sup>S153A</sup> showed moderate reduction of chemotaxis. In contrast to control cells, chemotaxis of these cells was not affected by FSK. These results are consistent with the role of VASP as a regulator of adhesion maturation and provide support for the hypothesis that altered adhesion dynamics impacts the ability of cells to establish stable protrusions and chemotaxis.

## DISCUSSION

In this study, we demonstrated that VASP phosphorylation by PKA is important for the regulation of focal adhesion growth, membrane ruffling, and chemotaxis of microglia cells toward ADP. Activation of P2Y<sub>12</sub> receptor by ADP stimulation caused the elevation of intracellular cAMP concentration. Mammalian genomes harbor nine distinct G protein coupled adenylyl cyclases (AC 1-AC 9)(Sunahara and Taussig, 2002; Tang and Hurley, 1998). The nine ACs show distinct expression profiles and modes of regulation by G proteins, calcium, and a variety of small molecules. Whereas all isoforms are stimulated by *Gas*, only AC 5 and AC 6 are sensitive to inhibition by *G $\alpha$ i*. In contrast, G $\beta\gamma$  can be either stimulatory, as for AC 2, AC 4, and AC 7, or inhibitory, as for AC 1 and AC 8 (Sunahara and Taussig, 2002; Tang and Hurley, 1998).

The activation of PKA presumably via the elevation of intracellular cAMP appears to be important for the ADP-induced chemotaxis and membrane ruffle formation as the PKA inhibitor blocked both. Growing evidence indicated that PKA is one of the major regulators for cell adhesion and migration. PKA is activated upon both cellular detachment and upon engagement of integrins (Howe and Juliano, 2000; O'Connor and Mercurio, 2001). Activation of PKA by FSH leads to filopodia and lamellipodia formation in granulose cells(Grieshaber et al., 2000). Both inhibition and hyper-activation of PKA inhibit cell migration (Edin et al., 2001; O'Connor and Mercurio, 2001). Stimulation of PKA pathway results in  $\beta$ 1Pix phosphorylation, which in turn controls  $\beta$ 1Pix translocation to focal complexes and Cdc42 activation(Chahdi et al., 2005).

VASP was first identified as a substrate of PKA and PKG which are regulated by cyclic nucleotides (Reinhard et al., 1992). VASP has three PKA/PKG phosphorylation sites: Ser157, Ser239, and Thr278 (residue numbers apply to human VASP; Ser153, Ser239, and Thr for mouse VASP)(Krause et al., 2003). Although each site can be modified by PKA and PKG, Ser157 is the preferred target for PKA and Ser239 is preferentially phosphorylated by PKG(Butt et al., 1994; Smolenski et al., 1998). It has been suggested that phosphorylation at these residues serves as an important regulatory mechanism for VASP function. As a major substrate for PKA, the VASP proteins coordinate different modes of actin organization including actin filament assembly, cross-linking, and bundling. In the myogenic cells, VASP phosphorylation by PKA inhibits actin polymerization from profilin-actin complexes

(Harbeck et al., 2000). Previous reports demonstrated that F-actin binding of VASP can be modulated by phosphorylation, resulting in the reduction of actin-polymerization-promoting activity (Harbeck et al., 2000), impaired actin stress fiber formation, and altered cell morphology (Blume et al., 2007). VASP family proteins localize to focal adhesion, largely through EVH1-mediated interaction with vinculin and zyxin (Krause et al., 2003; Renfranz and Beckerle, 2002; Rottner et al., 2001).

Cell locomotion is a dynamic process consisting of repeated cycles of protrusion of the leading edge, formation of new matrix adhesions, and retraction of the trailing edge (Carragher and Frame, 2004; Lauffenburger and Horwitz, 1996; Small et al., 1996; Webb et al., 2002). Interaction with ECM substrates stimulates integrin clustering and the formation of small transient integrin-associated FX, which are the initial sites of cell adhesion (Zimmerman et al., 2004). These events are usually followed by the formation of larger, more stable focal adhesions with tethered actin-stress fibers, which facilitate cell spreading and strengthening of adhesive links to the ECM. Modulating focal adhesion structure, by altering either the expression of certain focal adhesion components or the signaling pathways that regulate their assembly, and the dynamic regulation of their assembly and disassembly significantly affects cell migration (Carragher and Frame, 2004). Polar protrusions at the leading edge produce many FX, some of which develop into stable FA. FA, in turn, plays a dual role in motility; they provide robust anchors to the ECM, allowing the contractile actomyosin system to pull the cell body and trailing edge forward (Lauffenburger and Horwitz, 1996; Small et al., 1996) and they may also restrain the migration process (Huttenlocher et al., 1996). Our study is the first demonstration of the role of VASP proteins not only in the lamellipodial protrusion during membrane ruffling but also in the transformation of focal complexes into focal adhesions (FA) in microglia cells. Our results suggest that phosphorylation on Ser153 of VASP is required for the formation of focal complexes and protrusion of membranes, but inhibitory for the transformation of FX into FA. Dynamic regulation of VASP phosphorylation, thus, is essential for the chemotaxis of microglia. We also demonstrated how varying the surface coating concentration of FN substrate modulates persistent migration of microglia cells, and explored how adhesion-dependent changes in lamellipodial protrusion dynamics affects membrane ruffle formation and chemotaxis. These results provide evidence that protrusion and adhesion are closely coupled events in cell migration.

The extracellular nucleotides may play a role in modulating the microglial function of the brain in the early phase of pathology. Our study suggests that VASP function has an important role in the microglia chemotaxis through regulation of FA formation. These VASP functions are involved in the diverse functions of microglia, such as scavenging and neuroprotective actions, in pathological states.

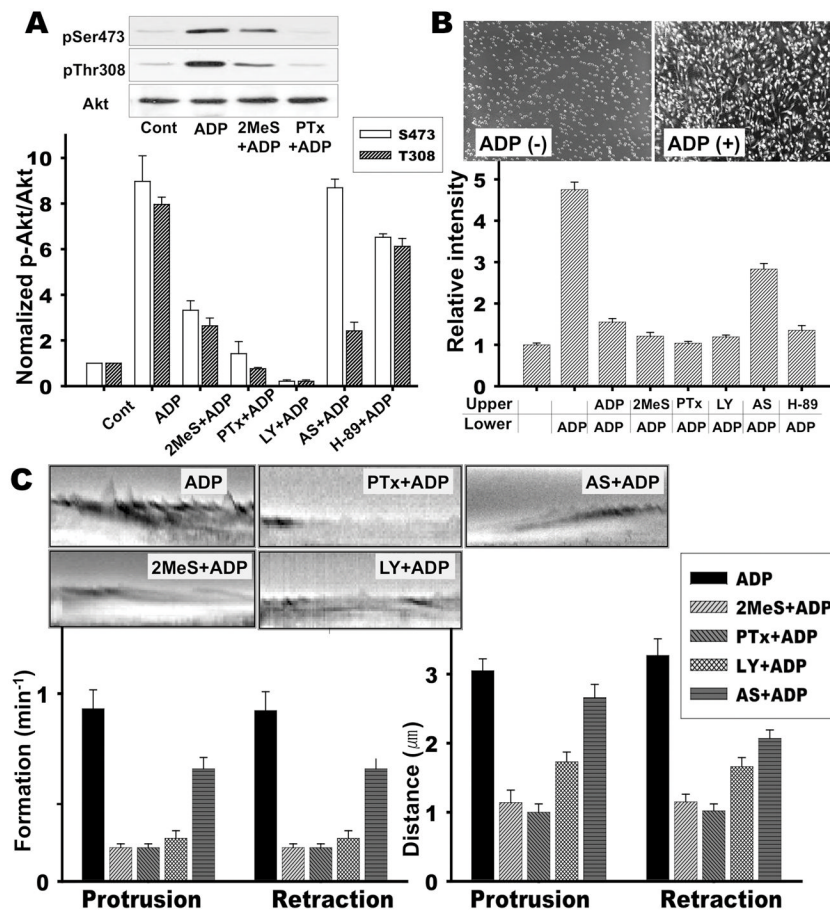
## References

- Bear JE, Svitkina TM, Krause M, Schafer DA, Loureiro JJ, Strasser GA, Maly IV, Chaga OY, Cooper JA, Borisy GG, Gertler FB. Antagonism between Ena/VASP proteins and actin filament capping regulates fibroblast motility. *Cell*. 2002; 109:509–521. [PubMed: 12086607]
- Blume C, Benz PM, Walter U, Ha J, Kemp BE, Renne T. AMP-activated protein kinase impairs endothelial actin cytoskeleton assembly by phosphorylating vasodilator-stimulated phosphoprotein. *J Biol Chem*. 2007; 282:4601–4612. [PubMed: 17082196]
- Borm B, Requardt RP, Herzog V, Kirfel G. Membrane ruffles in cell migration: indicators of inefficient lamellipodia adhesion and compartments of actin filament reorganization. *Exp Cell Res*. 2005a; 302:83–95. [PubMed: 15541728]
- Borm B, Requardt RP, Herzog V, Kirfel G. Membrane ruffles in cell migration: indicators of inefficient lamellipodia adhesion and compartments of actin filament reorganization. *Experimental Cell Research*. 2005b; 302:83–95. [PubMed: 15541728]

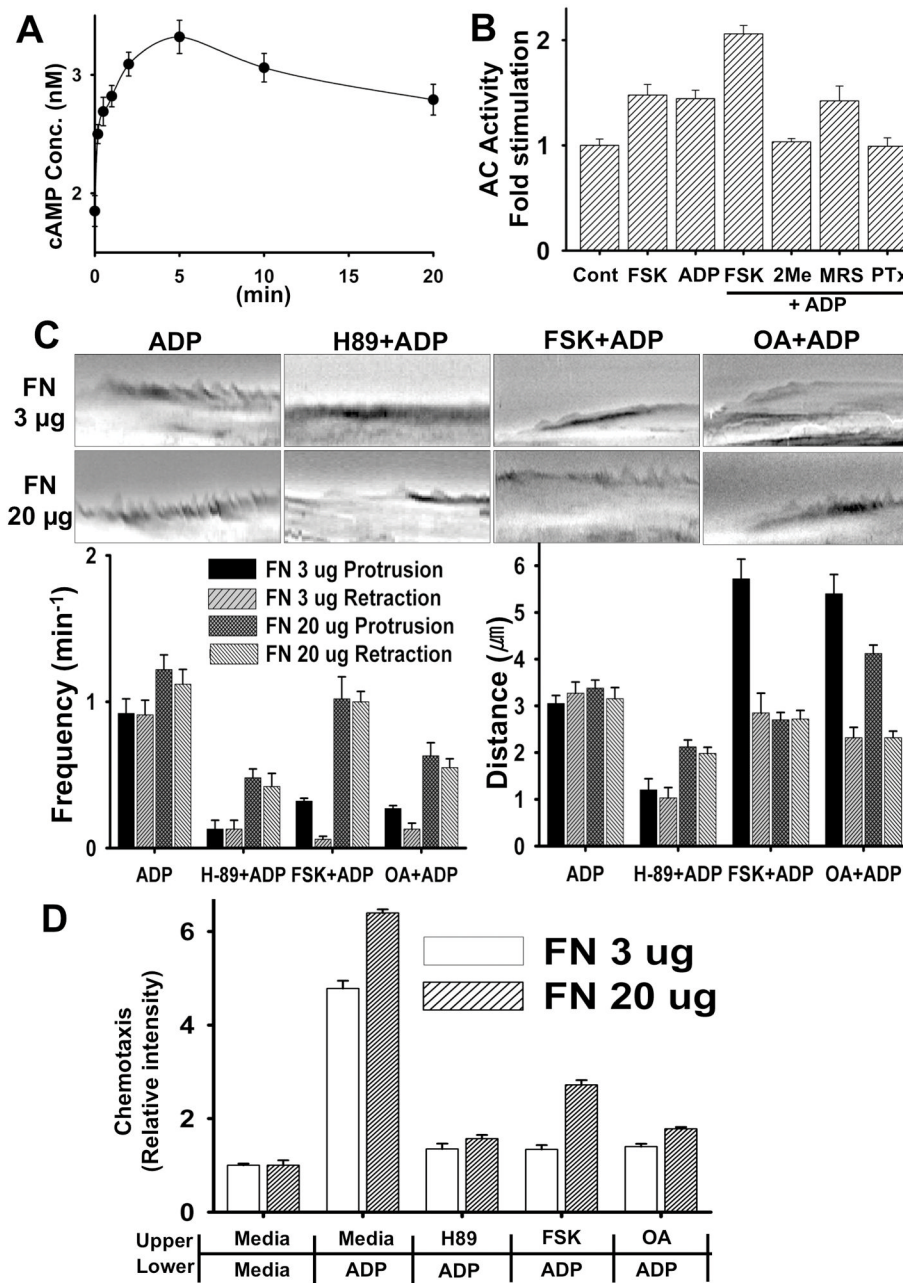


- Butt E, Abel K, Krieger M, Palm D, Hoppe V, Hoppe J, Walter U. cAMP- and cGMP-dependent protein kinase phosphorylation sites of the focal adhesion vasodilator-stimulated phosphoprotein (VASP) in vitro and in intact human platelets. *J Biol Chem.* 1994; 269:14509–14517. [PubMed: 8182057]
- Carragher NO, Frame MC. Focal adhesion and actin dynamics: a place where kinases and proteases meet to promote invasion. *Trends Cell Biol.* 2004; 14:241–249. [PubMed: 15130580]
- Chahdi A, Miller B, Sorokin A. Endothelin 1 Induces  $\beta$ 1Pix Translocation and Cdc42 Activation via Protein Kinase A-dependent Pathway. *J Biol Chem.* 2005; 280:578–584. [PubMed: 15513924]
- Chamak B, Mallat M. Fibronectin and laminin regulate the in vitro differentiation of microglial cells. *Neuroscience.* 1991; 45:513–527. [PubMed: 1663599]
- Critchley DR. Focal adhesions – the cytoskeletal connection. *Curr Opin Cell Biol.* 2000; 12:133–139. [PubMed: 10679361]
- Davalos D, Grutzendler J, Yang G, Kim JV, Zuo Y, Jung S, Littman DR, Dustin ML, Gan WB. ATP mediates rapid microglial response to local brain injury in vivo. *Nat Neurosci.* 2005; 8:752–758. [PubMed: 15895084]
- Dubyak GR, el-Moatassim C. Signal transduction via P<sub>2</sub>-purinergic receptors for extracellular ATP and other nucleotides. *Am J Physiol.* 1993; 265:C577–606. [PubMed: 8214015]
- Edin ML, Howe AK, Juliano RL. Inhibition of PKA blocks fibroblast migration in response to growth factors. *Exp Cell Res.* 2001; 270:214–222. [PubMed: 11640885]
- Gehrmann J, Matsumoto Y, Kreutzberg GW. Microglia: intrinsic immune effector cell of the brain. *Brain Res Brain Res Rev.* 1995; 20:269–287. [PubMed: 7550361]
- Griesshaber NA, Boitano S, Ji I, Mather JP, Ji TH. Differentiation of Granulosa Cell Line: Follicle-Stimulating Hormone Induces Formation of Lamellipodia and Filopodia via the Adenylyl Cyclase/Cyclic Adenosine Monophosphate Signal. *Endocrinology.* 2000; 141:3461–3470. [PubMed: 10965919]
- Hanisch UK. Microglia as a source and target of cytokines. *Glia.* 2002; 40:140–155. [PubMed: 12379902]
- Harbeck B, Huttelmaier S, Schluter K, Jockusch BM, Illenberger S. Phosphorylation of the vasodilator-stimulated phosphoprotein regulates its interaction with actin. *J Biol Chem.* 2000; 275:30817–30825. [PubMed: 10882740]
- Haynes SE, Hollopeter G, Yang G, Kurpius D, Dailey ME, Gan WB, Julius D. The P<sub>2</sub>Y<sub>12</sub> receptor regulates microglial activation by extracellular nucleotides. *Nat Neurosci.* 2006; 9:1512–1519. [PubMed: 17115040]
- Hickey WF. Basic principles of immunological surveillance of the normal central nervous system. *Glia.* 2001; 36:118–124. [PubMed: 11596120]
- Honda S, Sasaki Y, Ohsawa K, Imai Y, Nakamura Y, Inoue K, Kohsaka S. Extracellular ATP or ADP induce chemotaxis of cultured microglia through Gi/o-coupled P<sub>2</sub>Y receptors. *J Neurosci.* 2001; 21:1975–1982. [PubMed: 11245682]
- Howe AK, Juliano RL. Regulation of anchorage-dependent signal transduction by protein kinase A and p21-activated kinase. *Nat Cell Biol.* 2000; 2:593–600. [PubMed: 10980699]
- Huttenlocher A, Ginsberg MH, Horwitz AF. Modulation of cell migration by integrin-mediated cytoskeletal linkages and ligand-binding affinity. *J Cell Biol.* 1996; 134:1551–1562. [PubMed: 8830782]
- Inoue K. Microglial activation by purines and pyrimidines. *Glia.* 2002; 40:156–163. [PubMed: 12379903]
- Krause M, Dent EW, Bear JE, Loureiro JJ, Gertler FB. Ena/VASP proteins: regulators of the actin cytoskeleton and cell migration. *Annu Rev Cell Dev Biol.* 2003; 19:541–564. [PubMed: 14570581]
- Kreutzberg GW. Microglia: a sensor for pathological events in the CNS. *Trends Neurosci.* 1996; 19:312–318. [PubMed: 8843599]
- Lauffenburger DA, Horwitz AF. Cell migration: a physically integrated molecular process. *Cell.* 1996; 84:359–369. [PubMed: 8608589]

- Milner R, Campbell IL. Cytokines regulate microglial adhesion to laminin and astrocyte extracellular matrix via protein kinase C-dependent activation of the alpha6beta1 integrin. *J Neurosci*. 2002; 22:1562–1572. [PubMed: 11880486]
- Nasu-Tada K, Koizumi S, Inoue K. Involvement of beta1 integrin in microglial chemotaxis and proliferation on fibronectin: different regulations by ADP through PKA. *Glia*. 2005; 52:98–107. [PubMed: 15920726]
- Neary JT, Baker L, Jorgensen SL, Norenberg MD. Extracellular ATP induces stellation and increases glial fibrillary acidic protein content and DNA synthesis in primary astrocyte cultures. *Acta Neuropathol*. 1994; 87:8–13. [PubMed: 8140897]
- Nimmerjahn A, Kirchhoff F, Helmchen F. Resting microglial cells are highly dynamic surveillants of brain parenchyma in vivo. *Science*. 2005; 308:1314–1318. [PubMed: 15831717]
- O'Connor KL, Mercurio AM. Protein kinase A regulates Rac and is required for the growth factor-stimulated migration of carcinoma cells. *J Biol Chem*. 2001; 276:47895–47900. [PubMed: 11606581]
- O'Connor KL, Shaw LM, Mercurio AM. Release of cAMP gating by the alpha6beta4 integrin stimulates lamellae formation and the chemotactic migration of invasive carcinoma cells. *J Cell Biol*. 1998; 143:1749–1760. [PubMed: 9852165]
- Ohsawa K, Irino Y, Nakamura Y, Akazawa C, Inoue K, Kohsaka S. Involvement of P2X4 and P2Y12 receptors in ATP-induced microglial chemotaxis. *Glia*. 2007; 55:604–616. [PubMed: 17299767]
- Reinhard M, Halbrugge M, Scheer U, Wiegand C, Jockusch BM, Walter U. The 46/50 kDa phosphoprotein VASP purified from human platelets is a novel protein associated with actin filaments and focal contacts. *Embo J*. 1992; 11:2063–2070. [PubMed: 1318192]
- Renfranz PJ, Beckerle MC. Doing (F/L)PPPPs: EVH1 domains and their proline-rich partners in cell polarity and migration. *Curr Opin Cell Biol*. 2002; 14:88–103. [PubMed: 11792550]
- Rottner K, Krause M, Gimona M, Small JV, Wehland J. Zyxin is not colocalized with vasodilator-stimulated phosphoprotein (VASP) at lamellipodial tips and exhibits different dynamics to vinculin, paxillin, and VASP in focal adhesions. *Mol Biol Cell*. 2001; 12:3103–3113. [PubMed: 11598195]
- Sasaki Y, Hoshi M, Akazawa C, Nakamura Y, Tsuzuki H, Inoue K, Kohsaka S. Selective expression of Gi/o-coupled ATP receptor P2Y12 in microglia in rat brain. *Glia*. 2003; 44:242–250. [PubMed: 14603465]
- Small JV, Anderson K, Rottner K. Actin and the coordination of protrusion, attachment and retraction in cell crawling. *Biosci Rep*. 1996; 16:351–368. [PubMed: 8913526]
- Smolenski A, Bachmann C, Reinhard K, Honig-Liedl P, Jarchau T, Hoschuetzky H, Walter U. Analysis and regulation of vasodilator-stimulated phosphoprotein serine 239 phosphorylation in vitro and in intact cells using a phosphospecific monoclonal antibody. *J Biol Chem*. 1998; 273:20029–20035. [PubMed: 9685341]
- Stence N, Waite M, Dailey ME. Dynamics of microglial activation: a confocal time-lapse analysis in hippocampal slices. *Glia*. 2001; 33:256–266. [PubMed: 11241743]
- Streit WJ. Microglia as neuroprotective, immunocompetent cells of the CNS. *Glia*. 2002; 40:133–139. [PubMed: 12379901]
- Sunahara RK, Taussig R. Isoforms of mammalian adenylyl cyclase: multiplicities of signaling. *Mol Interv*. 2002; 2:168–184. [PubMed: 14993377]
- Tang WJ, Hurley JH. Catalytic mechanism and regulation of mammalian adenylyl cyclases. *Mol Pharmacol*. 1998; 54:231–240. [PubMed: 9687563]
- Thomas WE. Brain macrophages: on the role of pericytes and perivascular cells. *Brain Res Brain Res Rev*. 1999; 31:42–57. [PubMed: 10611494]
- Van Kolen K, Slegers H. Integration of P2Y receptor-activated signal transduction pathways in G protein-dependent signalling networks. *Purinergic Signal*. 2006; 2:451–469. [PubMed: 18404483]
- Webb DJ, Parsons JT, Horwitz AF. Adhesion assembly, disassembly and turnover in migrating cells -- over and over and over again. *Nat Cell Biol*. 2002; 4:E97–100. [PubMed: 11944043]
- Zimmerman B, Volberg T, Geiger B. Early molecular events in the assembly of the focal adhesion-stress fiber complex during fibroblast spreading. *Cell Motil Cytoskeleton*. 2004; 58:143–159. [PubMed: 15146534]

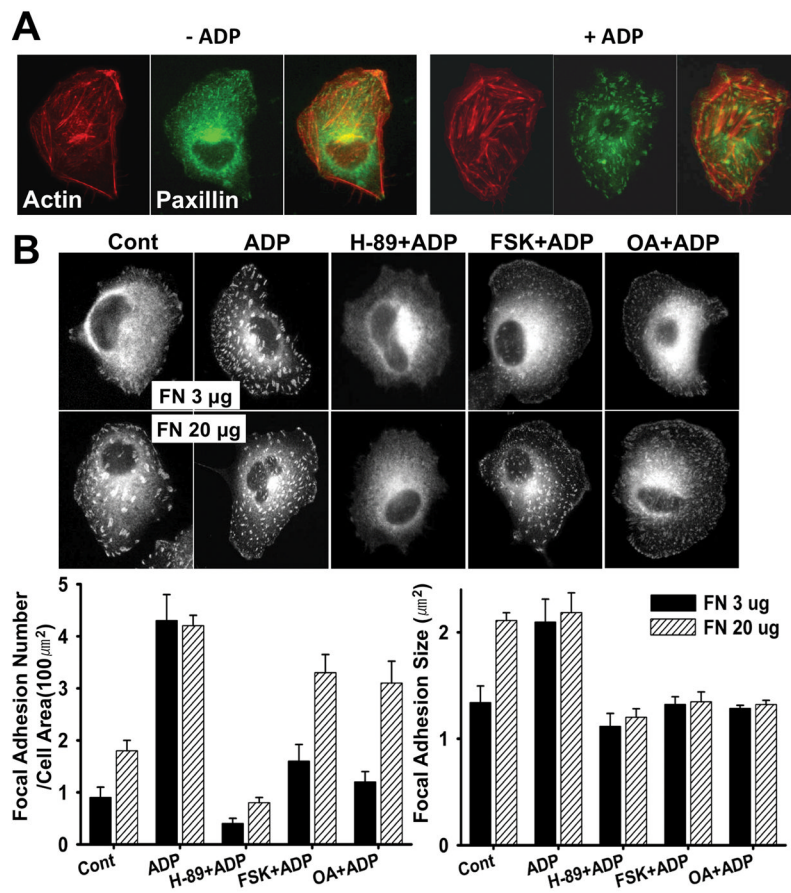


**Figure 1.** Role of the P2Y12-dependent activation of PI3K for ADP-induced chemotaxis and membrane ruffle formation. **A.** Phosphorylation of Akt on Thr308 or Ser473 upon ADP stimulation. BV2 cells were pretreated with 50  $\mu$ M 2MeSAMP for 10 min, 100 ng/ml Pertussis toxin for 4 hr, 20  $\mu$ M LY294002, 10  $\mu$ M AS604850, or 30  $\mu$ M H-89 for 20 min. Cells were then stimulated with 100  $\mu$ M ADP for 5 min. Cells were lysed and subjected to western blot by anti-pAkt (S473 and T308) and anti-Akt antibody. Quantification of Akt activation from five independent experiments were shown in the bottom panel. Error bars indicate  $\pm$  SEM. **B.** Cells were assayed for migration toward 100  $\mu$ M ADP in the continued presence of these inhibitors using a Transwell chamber assay as described under “Materials and Methods”. Cells that migrated to the bottom of the polycarbonate membrane were stained with crystal violet (top panel picture) and quantifications using *Image Quant* software from three independent experiments are shown in the bottom panel figure. **C.** Lamella dynamics was analyzed by kymographs. For each group, membrane ruffles of at least 10 individual cells were monitored over a 15 min period by capturing digital images every 6 seconds. Subsequently, three areas of interest were marked on each image by lines that cross the cell lamella. Kymographs were assembled using *MetaMorph* software. Representative kymographs are shown and quantifications of ruffle formation from five independent experiments are shown.



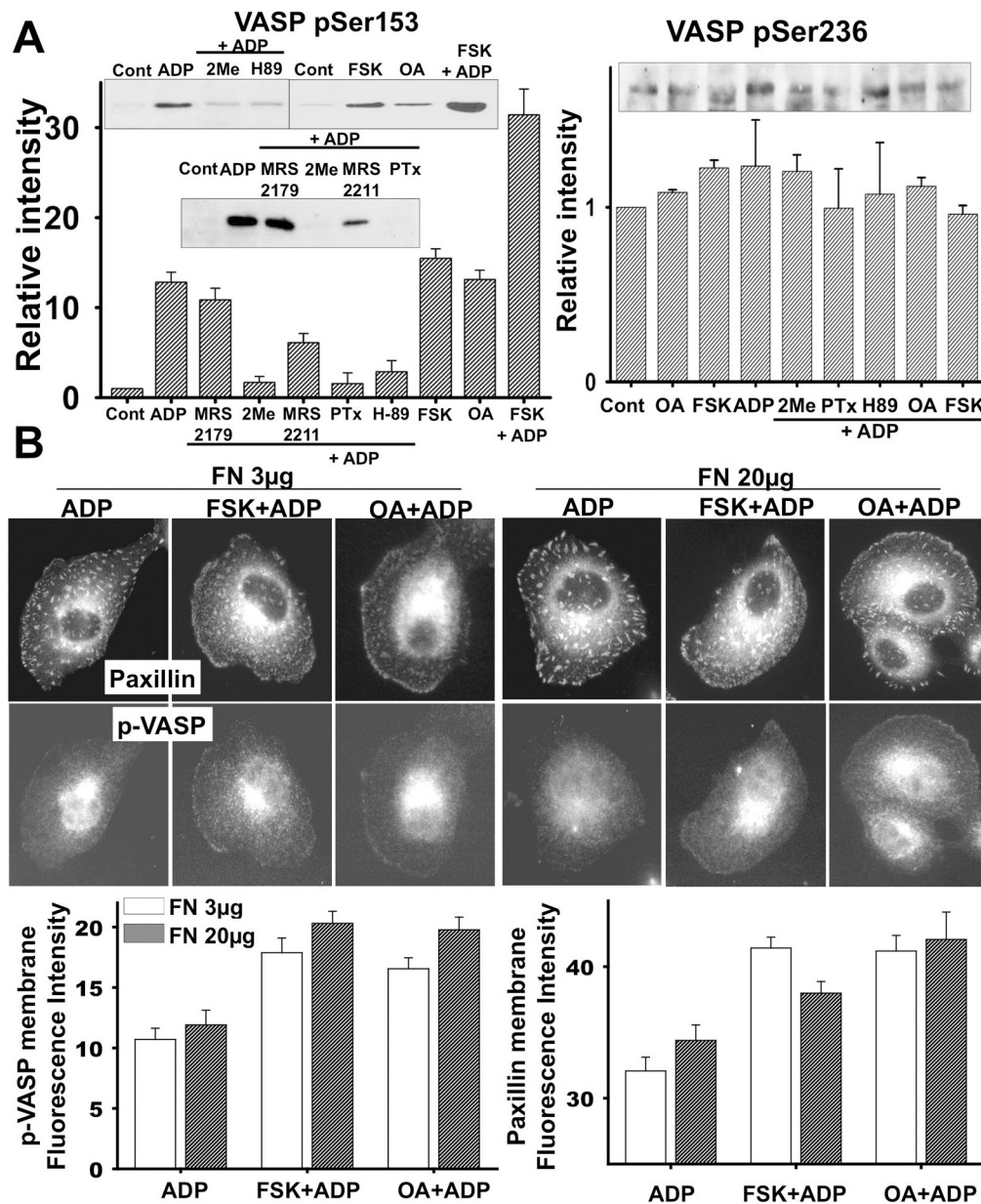
**Figure 2.** (A) ADP transiently stimulates Adenylyl Cyclase (AC) activity. BV2 cells were stimulated with 100 μM ADP for the time indicated and then cAMP concentration was measured with CatchPoint Cyclic-AMP fluorescent Assay kit. (B) ADP-induces AC activation through the Gi/o-coupled P2Y12 receptor. BV2 cells that were pretreated with inhibitors and cells were then lysed and subjected to cAMP assay. (C) FSK, OA, and H-89 have an inhibitory effect on ADP-induced membrane ruffling. Cells were pretreated with 10 μM FSK, 1 μM Okadaic acid (OA) or 30 μM H-89 for 20 min and then stimulated with 100 μM ADP. Lamella dynamics was then analyzed by kymographs. (D) FSK, OA, and H-89 have an inhibitory effect on ADP-induced chemotaxis of microglia cells. Transwell chamber membranes were coated with 3 μg/ml or 20 μg/ml fibronectin for 8 hr. Cells were then assayed for migration

toward 100  $\mu$ M ADP in the continued presence of H-89, FSK and OA. Averages of five independent experiments are shown.



**Figure 3.**

(A) Increase of focal adhesions and stress fibers upon ADP stimulation. F-actin and paxillin were stained with phalloidin and anti-paxillin antibody. (B) Cells were plated on coverslips coated with 3 or 20 µg/ml fibronectin. After pretreatment with FSK, OA, or H-89 for 20 min, cells were stimulated with 100 µM ADP for 5 min. Immunostaining was performed on fixed cells with anti-mouse paxillin antibody. The size and number of focal adhesions were measured from the images (n=20). Error bars indicate ± SEM.

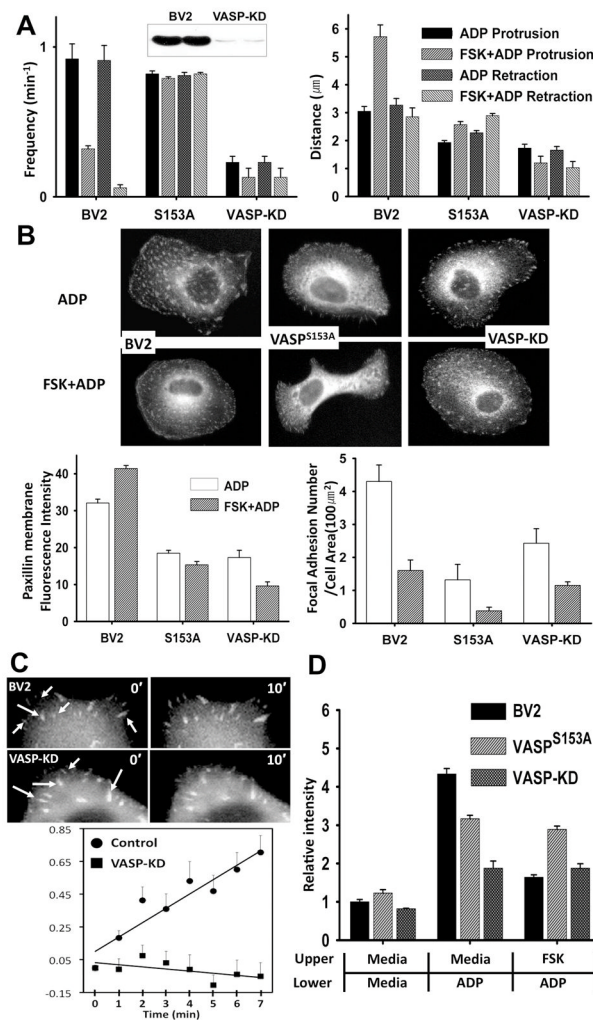


**Figure 4.**

Prolonged phosphorylation of VASP inhibits the transformation of focal complexes into focal adhesion, retraction of membrane ruffles, and chemotaxis. (A) VASP phosphorylation on Ser<sup>157</sup> or Ser<sup>239</sup> was examined by immunoblots. Cells were incubated with pharmacological agents at the concentrations indicated for 20 min and then stimulated with ADP for 5 min. Cells were then lysed and phosphorylation of VASP was detected by western blot analysis with anti-pVASP (S157 or S239) antibody. Representative blots in insets and quantifications of pVASP band intensities from three independent experiments are shown. (B) Immunostaining of paxillin and pVASP (S157) in cells treated with FSK and OA. Coverslips were coated with 3 or 20  $\mu$ g/ml fibronectin for 1 hr and cells were plated. Cells were pretreated with 10  $\mu$ M FSK or 1  $\mu$ M OA for 20 min and then stimulated with 100  $\mu$ M ADP for 5 min. Immunostaining was performed on fixed cells with mouse anti-paxillin

and rabbit anti-pVASP (S157) antibody Fluorescence intensities of pVASP and paxillin along the membrane, quantified from the images, are shown in the graphs.



**Figure 5.**

(A) Membrane ruffle formation in VASP knock-down (VASP-KD) or cells expressing non-phosphorylatable VASP mutant (VASP<sup>S153A</sup>-GFP). Inset shows the reduction of VASP in VASP-KD cells detected by western blot analysis. (B) Changes in the number of focal complexes or adhesions examined by paxillin immunostaining in VASP-KD cells and cells expressing VASP<sup>S153A</sup>-GFP. (C) Time series of GFP-paxillin-marked adhesion assembly of VASP-KD cells were acquired at 1 min intervals for 20 min and images at 0 min and 10 min are shown. Arrows indicate adhesions. Fluorescence intensities of adhesions at each time point were measured. Points represent average + SEM of the natural log of the ratio of the integrated fluorescent intensity at each time point to the initial fluorescent intensity. Measurements were performed on 10 to 15 individual adhesions from 5–7 cells. (D) Chemotaxis of VASP-KD cells or cells expressing VASP<sup>S153A</sup>-GFP. Transwell chamber membranes were coated with 3  $\mu$ g/ml fibronectin for 1 hr and cells were plated. Cells were then assayed for migration toward 100  $\mu$ M ADP in the continued presence of FSK or OA.